

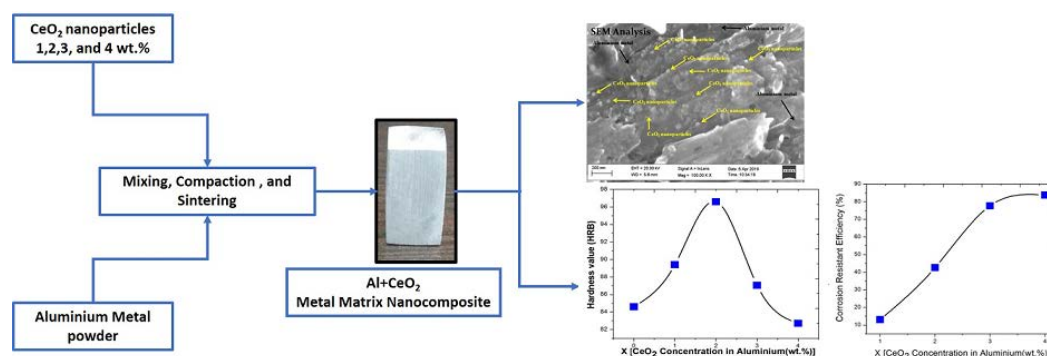
Mechanical and structural properties of aluminium nanocomposites reinforced with cerium oxide nanoparticles fabricated by powder metallurgy

Naveen Kumar,¹ Kumar Navin,¹ Richard J. Ball,² Rajnish Kurchania^{1*}

¹Functional Nanomaterials Laboratory, Nanoscience & Engineering Centre, Department of Physics, Maulana Azad National Institute of Technology (MANIT), Bhopal-462003. Madhya Pradesh, India. ²BRE Centre for Innovative Construction Materials, Department of Architecture and Civil Engineering, University of Bath, Bath, BA2 7AY, UK.

Submitted on: 12-Oct-2020, Accepted on: 22-Nov-2020, Published on: 27-Nov-2020

ABSTRACT



The metal matrix nanocomposites were synthesized by the powder metallurgy method with Ceria (CeO₂) nanoparticles (1, 2, 3, 4 wt.%) as reinforcement contained within an Aluminium (Al) metal matrix. The structural and mechanical properties of the concentration of reinforced CeO₂ nanoparticles. The Ceria nanoparticles were synthesized by using the Co-precipitation technique with a face-centered cubic (fcc) structure with an average crystallite size of 12.80 nm. The structural analysis of the nanocomposites confirms the uniform dispersion of CeO₂ nanoparticles in an Al matrix. There is a significant development in the hardness value of Al due to the CeO₂ nanoparticles and the maximum hardness value was obtained for 2 wt. % of CeO₂ in the Al matrix, while an increase in the wear of the Al-CeO₂ nanocomposites was observed as compared to pure aluminium. The corrosion analysis also confirms the improvement in the corrosion resistance of the Al-CeO₂ nanocomposite with a maximum corrosion resistance efficiency of 83.75 % for 4 wt.% CeO₂ in the Al matrix..

Keywords: Co-precipitation, CeO₂ nanoparticles, metal matrix nanocomposites (MMNCs), corrosion resistance, hardness

INTRODUCTION

The metal matrix reinforced with nanoparticles is called metal matrix nanocomposites (MMNCs). Nowadays, because of their superior and excellent properties over conventional materials, they are under serious consideration to substitute conventional

materials. Nanoparticle reinforcement improves specific stiffness, strength, creep resistance, and thermal conductivity due to the interaction of the reinforcement phase with dislocations.¹ Several types of MMNCs were reported earlier, such as Fe-MgO, W-Cu, Mg-TiC, and Fe-TiC and they have better mechanical properties like toughness as compared to conventional material.²⁻⁵ Generally, when the metal matrix is reinforced with some ceramic material, due to the high expansion of the metal and the low expansion of the ceramic, there is a thermal mismatch which results in dislocations and cracks when cooling the matrix material.⁶ There are several methods available for the fabrication of nanocomposites such as stir casting, powder metallurgy, high energy ball milling, and diffusion bonding.⁷ In the stir casting

*Corresponding Author Name: Dr. Rajnish Kurchania
Tel: +91 755 4051595 Fax: +91 755 2670562
Email: rkurchania@gmail.com

Cite as: *J. Mat. NanoSci.*, 2020, 7(2), 73-78

©The ScienceIn ISSN 2394-0867
<http://pubs.thesciencein.org/jmns>

method, the matrix material is melted into a liquid state, and then reinforcing particles are introduced into the liquid matrix. The properties of the metal matrix in stir casting can be altered by variable parameters such as pour temperature, preheat temperature, stirring speed, retention time, etc. In the powder metallurgy method, the reinforced particle is mixed with a metal matrix and pressed into the desired shape by compaction and heat treatment. This method has the advantage of fewer defects such as shrinkage and porosity.⁸

Aluminium is one of the most popular matrix materials for the MMNCs. Aluminium matrix nanocomposites (AMNC) are considered today as a substitute for conventional materials due to their large number of applications in structural and mechanical areas such as aerospace, aeronautics, defense, and shipbuilding industries due to their superior properties. They are industrialized to meet the demands of lighter materials that have high strength, high rigidity, and good wear resistance. Aluminium is the most widely used non-ferrous metal and is often reinforced with a variety of materials to improve its mechanical properties, such as Al-C60, Al-Al₂O₃, Al-Mg-Si, Al-Graphene, Al-B₄C, and Al-ZrO₂.⁹⁻¹⁶ Aluminium reinforced with nano-sized lead particles improves friction and wear characteristics because the lead layer reduces the coefficient of friction.¹⁷ It has been reported that the Al-SiC composite with mesh-like structure has a low density, high elastic modulus, low coefficient of thermal expansion and high conductivity.¹⁸ High strength aluminium reinforced with Multi-walled carbon nanotubes (MWCNTs) by powder metallurgy method followed by hot extrusion, significant improvements in the density, hardness value, and tensile strength.¹⁹

Aluminium is a very reactive metal and has a very high affinity towards oxygen and due to this, a layer of aluminium oxide is formed over the surface of the Al. Because of this phenomenon, it is extremely resistant to corrosion under a variety of environments and chemical reagents.²⁰ This makes aluminium and its alloys highly useful for aerospace, transportation, food packaging and building industries. Despite aluminium being corrosive resistant, aluminium tends to corrode in the marine environment because of simultaneous anodic and cathodic reactions on the metal surface leading to generation of electrical charge on metal.²⁰⁻²²

Ceria nanoparticles (CeO₂) are one of the most promising materials. It is an interesting material for solid oxide fuel cells due to its high oxygen ion conductivity. Ceria also increases the electronic conductivity of materials under reducing conditions. Moreover, it is also used for automotive applications as catalytic converters.²² CeO₂ is one of the potential materials for the protection of metals from corrosion because cerium compounds show more negative potentials which makes it an extremely good cathodic inhibitor. Different methods have been reported for the synthesis of CeO₂ nanoparticles which are co-precipitation, flame spray pyrolysis, a microwave-assisted heating technique, and hydrothermal synthesis.²³⁻²⁷

In this work, CeO₂ nanoparticles were synthesized by co-precipitation technique and reinforced with an Al matrix by 1, 2, 3, and 4 wt.% to fabricate MMNCs by powder metallurgy method. The microstructural, mechanical, and corrosion properties of these MMNCs have been studied.

EXPERIMENTAL

Synthesis of cerium oxide nanoparticles

Cerium (III) nitrate [Ce(NO₃)₃•6H₂O] is used as a precursor for the synthesis of ceria nanoparticles and de-ionized water as a solvent. Initially, the 0.02M solution of cerium (III) nitrate is prepared by vigorously stirring for 1 hour, and then 0.01M ammonium hydroxide [NH₄OH] solution is added dropwise and immediately the light brown precipitates of Ce(OH)₃ are formed. When pH value reaches 10, the colour of precipitate changes to purple which shows the complete conversion of Ce(OH)₃ to Ce(OH)₄. Now the reaction is stopped after vigorous stirring for 3 hours. Now the purple precipitate is washed and centrifuged with de-ionized water and ethanol several times. When the purple precipitate is washed with ethanol the precipitate slowly changes its colour to light yellow. The precipitate is washed and centrifuged with ethanol until the colour completely changes to yellow. The yellow colour precipitate formed is the confirmation of the CeO₂ nanoparticles. Now the yellow precipitate is separated, dried at 100°C for 3 hours and then calcinated at 600°C for 3 hours to obtain CeO₂ nanoparticles.

Fabrication of Al-CeO₂ nanocomposite

The Al metal powder (99.99% purity, AR, CDH) as a metal matrix material and the CeO₂ nanoparticle synthesized by co-precipitation technique were mixed with different concentrations (1, 2, 3 & 4wt.%) of CeO₂ nanoparticles. The mixture was ground thoroughly with the help of a grinder so that the nanoparticles are uniformly mixed with the aluminium powder. Subsequently, these powdered samples were pressed with the help of the hydraulic press and die into the desired shape by applying a load of 30 kN and four pellets of different concentrations of CeO₂ were obtained. After that, these pellets were sintered at 635°C for 3 hours in the muffle furnace and allow to cool to room temperature in the furnace.²⁸ After cooling silvery-white colored solid materials were obtained, which are the nanocomposites of aluminium metal and cerium oxide.

Characterization

X-Ray Diffraction (PANalytical Empyrean) was used for the structural analysis of pure CeO₂, Al metal, and Al-CeO₂ nanocomposites using Cu-K α radiation ($\lambda = 1.5418\text{\AA}$) in the range of $2\theta = 20^\circ$ to 80° . A field emission scanning electron microscope (FESEM, Zeiss-ULTRA Plus) is used for the microstructural studies of the sintered nanocomposites. Rockwell hardness values of the nanocomposites were obtained by using the ball indenter of $\frac{1}{16}''$ at 100 Kg load on digital hardness testing machine. Dry sliding wear test was carried out on a pin-on-disc wear machine where test parameters were pin diameter of the specimen was 8mm, rpm of the disc was 425 rpm, the radial distance was 30mm and the load was 30 N. Electrochemical analysis (corrosion test) for nanocomposites is performed by Tafel extrapolation using three-electrode electrochemical analyzer (CHI-604D) and 3.5% NaCl solution as an electrolyte. The working electrodes were prepared from pure aluminium and Al-CeO₂ nanocomposite (10mm×5mm×1mm), Ag/AgCl wire as a reference electrode and platinum wire as a counter electrode with a 0.01 V/s scan rate.

RESULTS AND DISCUSSIONS

Structural analysis

Figure 1 shows the XRD Pattern of pure Al and CeO₂ nanoparticles synthesized by co-precipitation technique. The XRD pattern confirms the formation of CeO₂ nanoparticles with fcc structure (JCPDS No. 43-1002) without any impurity phase. The average crystallite size obtained is 12.80 nm by using the Debye-Scherrer formula which is mentioned below.

$$D = \frac{k\lambda}{\beta \cos \theta} \quad (1)$$

Where β = Full Width Half Maxima (radian), k = shape factor (0.9), $\lambda = 1.5418\text{\AA}$, D = Avg. crystallite size, θ = Half of the angle at which the highest peak occurs ($^{\circ}$). The XRD pattern of Al confirms the fcc structure (JCPDS No. 85-1372) without any impurity phase. The average crystallite size obtained is 31.27nm. Figure 2 shows the XRD pattern of the metal matrix nanocomposite with different wt % of the ceria nanoparticles. The XRD data shows the presence of CeO₂ nanoparticles and Al in the nanocomposite and each phase appears separately which confirms the formation of the nanocomposite. The peaks of Al metal are marked with '*' and the CeO₂ peak is marked with '#' in the XRD data of nanocomposite. The average crystallite sizes of the Al phase is calculated along the (111) plane of the aluminium peak

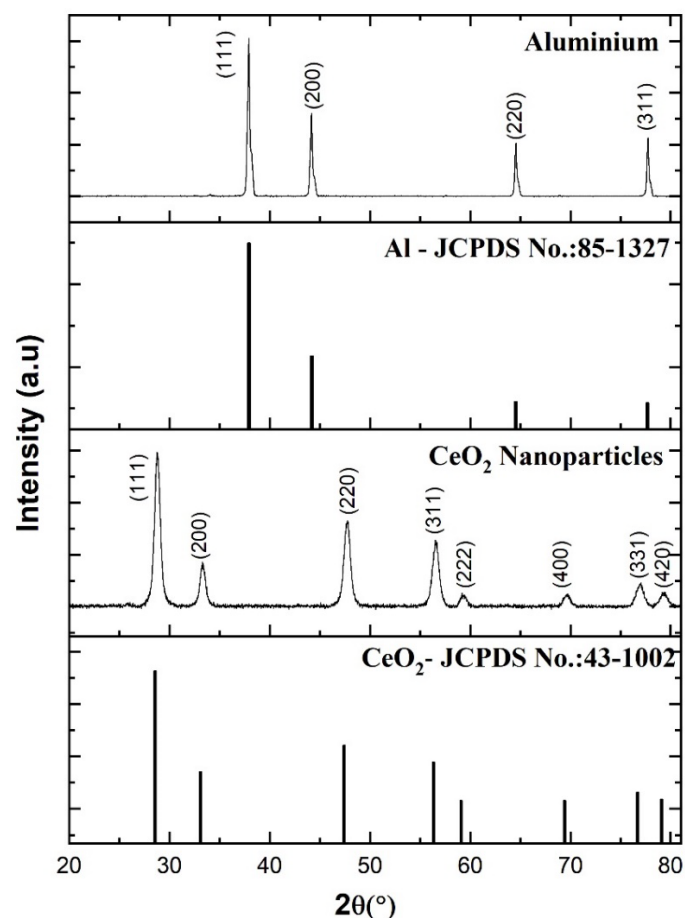


Figure 1. XRD graph of CeO₂ synthesized by co-precipitation method and Al metal along with JCPDS card.

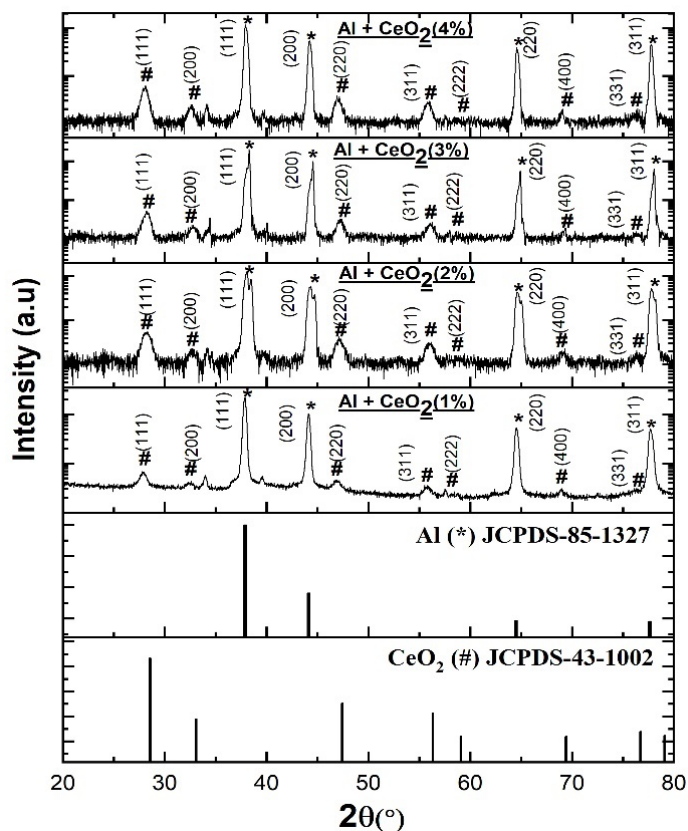


Figure 2. XRD graph of Al MMNCs reinforced with different wt.% of CeO₂.

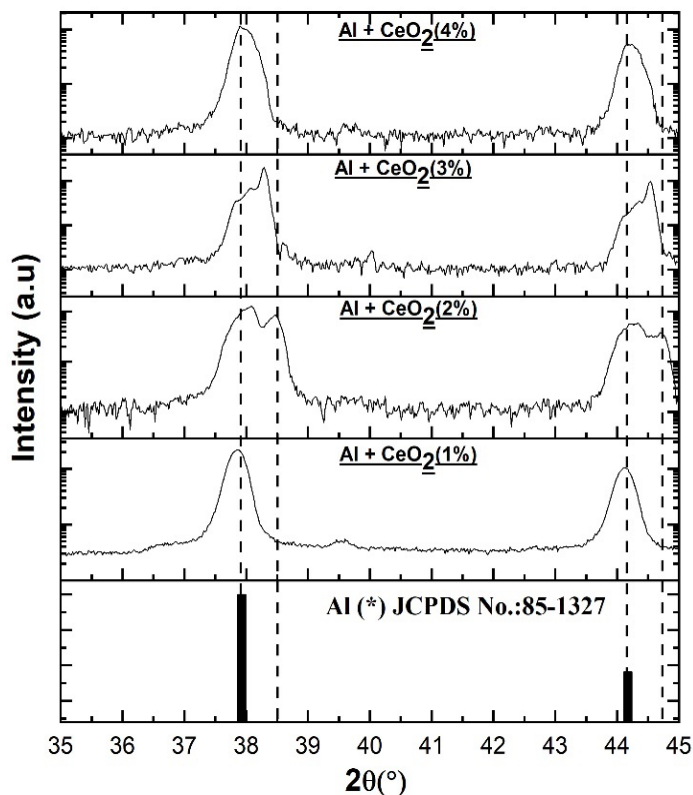
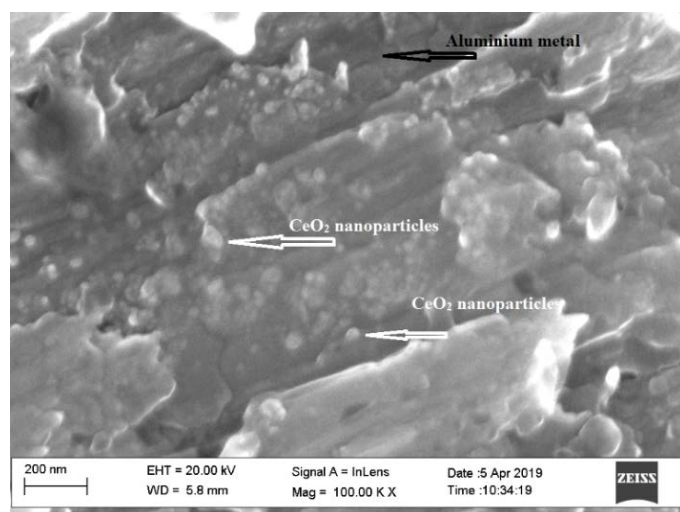


Figure 3. Enlarged view of XRD pattern of nanocomposite in 2 θ range (35 $^{\circ}$ to 45 $^{\circ}$).

Table 1. Average crystallite sizes of CeO₂ and Al-MMNCs on reinforcement of different wt.% of CeO₂.

Sample Details	Crystal Structure	Crystallite Size (nm)
CeO ₂	FCC	12.80
Aluminium	FCC	31.27
Al+CeO ₂ (1wt.%)	FCC	26.89
Al+CeO ₂ (2wt.%)	FCC	11.17
Al+CeO ₂ (3wt.%)	FCC	58.46
Al+CeO ₂ (4wt.%)	FCC	23.46

**Figure 4.** FESEM image of nanocomposite showing CeO₂ nanoparticles.

are 26.89nm, 11.17nm, 58.46nm, and 23.46nm for 1, 2, 3 & 4wt.% of CeO₂ concentrations in Al which are mentioned in Table 1. Figure 3 shows the XRD pattern in the 2 θ range of 35° to 45° in which shifting in the peaks of aluminium can be observed with different CeO₂ concentrations. This is mainly because of the change in lattice parameters due to the development of residual stress caused by sintering and partial dissolution of CeO₂ nanoparticles in aluminium.²⁹ Figure 4 shows the microstructural analysis of Al-CeO₂ nanocomposite (Al+2 wt.% CeO₂). The dark portion in the microscopic image is aluminium metal marked with a black colored arrow and the CeO₂ reinforcement particles can be seen as a white portion marked with a white-colored arrow. The image shows proper interfacial bonding between aluminium and CeO₂ particles. The CeO₂ nanoparticles are surrounded by aluminium solids and the uniform reinforcement of CeO₂ nanoparticles.

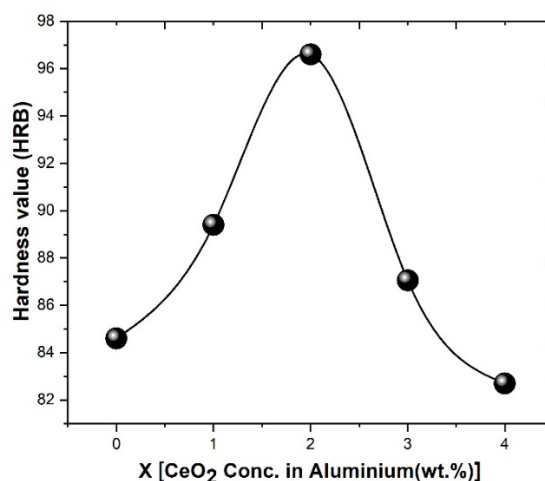
Mechanical properties

Rockwell hardness test of the pellet specimens was carried out on the hardness testing machine with a 1/16" ball indenter is used for the indentation purpose. The test was carried out at 100 Kg of load and the hardness values obtained are 84.6 for pure Al metal and 89.4, 96.4, 87.05, and 82.7 for nanocomposites of 1, 2, 3 & 4 wt.% of CeO₂ concentrations respectively which is

summarized in Table 2. Figure 5 shows the variation hardness for different specimens with the change in CeO₂ concentration. The hardness of the Al increases with CeO₂ concentration and maximum hardness value was obtained for 2 wt.% of CeO₂ concentration. Because of the uniform distribution of CeO₂ in the matrix, nano CeO₂ resists the movement of dislocations present in Al-matrix which results in increased hardness value. But, when the CeO₂ concentration is more than 2 wt.%, then the agglomeration of CeO₂ nanoparticles at grain boundaries takes place in the Al-matrix, which decreases the hardness value. Similar results have been reported for Al-Al₂O₃.³⁰ A dry sliding wear test for a specimen having a pin diameter of 8mm was carried out on a pin-on-disc wear machine at 30N of load with a radial distance of 30mm and the rpm of the disc was 425 rpm. Figure 6 shows the variation in average values of wear, frictional force and coefficient of friction obtained for pure Al metal and Al-CeO₂ nanocomposites and values are mentioned in Table 2. From the

Table 2. Hardness value, avg. wear, avg. frictional force, avg. coefficient of friction, corrosion current and corrosion resistance efficiency values for Al MMNCs.

Sample Details	Rockwell Hardness Value (HRB)	Avg. Wear (micro ns)	Avg. Frictional Force (N)	Avg. Coefficient of Friction	I _{corr} (μ A)	Corrosion Resistance Efficiency η (%)
Aluminium	84.6	69.30	13.54	0.46	77.44	-
Al+CeO ₂ (1wt.%)	89.4	397.18	19.94	0.68	67.29	13.10
Al+CeO ₂ (2wt.%)	96.6	292.82	12.32	0.41	44.46	42.58
Al+CeO ₂ (3wt.%)	87.05	357.51	13.53	0.45	17.29	77.67
Al+CeO ₂ (4wt.%)	82.7	328.64	13.23	0.4315	12.58	83.75

**Figure 5.** Variation of CeO₂ nanoparticles in Al metal matrix with hardness value.

results of the wear test, it is observed that Al-CeO₂ nanocomposites suffer more wear as compared to pure Al metal. This increase in wear can be attributed to the debris formed during the wear test which further acts as an abrasive particle to both the surfaces.³¹ However, frictional force and coefficient of friction increase and decrease alternatively with different wt.% of CeO₂. The coefficient of friction is directly proportional to frictional force so it changes in the same way as frictional force change.

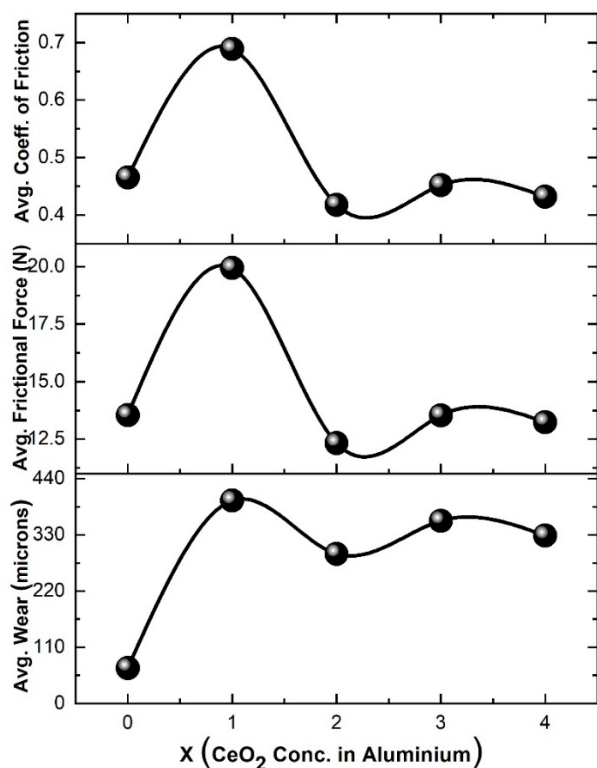
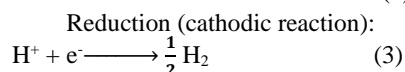
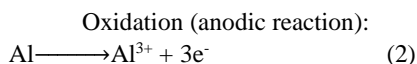


Figure 6. Variation of CeO₂ nanoparticles in Al metal matrix with avg. wear, avg. frictional force and avg. coefficient of friction.

Electrochemical analysis (corrosion test)

Aluminium corrodes because of simultaneous anodic and cathodic reactions on the Al metal surface in the presence of ionic solution.



The electrochemical technique is used for the determination of the corrosion resistance efficiency of the nanocomposite specimens over pure aluminium³²⁻³⁴. Figure 7(a) shows the Tafel plot obtained for different specimens, which shows the decrement in the corrosion current with the increment of CeO₂ concentration because CeO₂ nanoparticles are surrounded by aluminium particles and the CeO₂ nanoparticles act as a cathodic inhibitor.³⁵ Cerium has a high affinity for oxygen.³⁶ The existed bond between cerium and oxygen can be broken down under cathodic potential. Due to the bond breakage, the cerium ions are formed which leads to the formation of insoluble hydroxides which resist the flow of current in aluminium suppressing the corrosion. The corrosion

resistance efficiency is calculated with the use of the formula mentioned below.

$$\eta\% = \frac{I_{\text{corr}} - I'_{\text{corr}}}{I_{\text{corr}}} \times 100 \quad (4)$$

Where, I_{corr} = corrosion current for aluminium and I' _{corr} = corrosion current for nanocomposites. By interchanging the axes of the Tafel plot with each other and using Tafel extrapolation corrosion current is determined which is mentioned in Table 2. Figure 7(b) shows that, as we increase the CeO₂ concentration in aluminium the ability of aluminium to resist corrosion is increased.

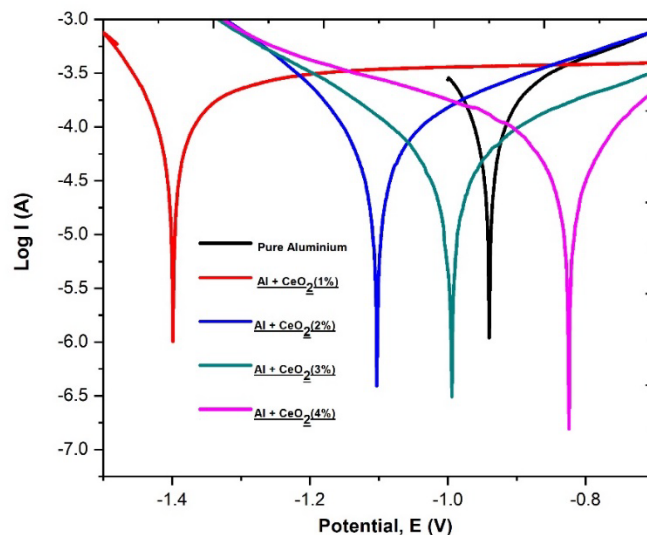


Figure 7(a). Tafel plots for Al matrix in 3.5% NaCl with and without CeO₂ nanoparticles in Al MMNCs.

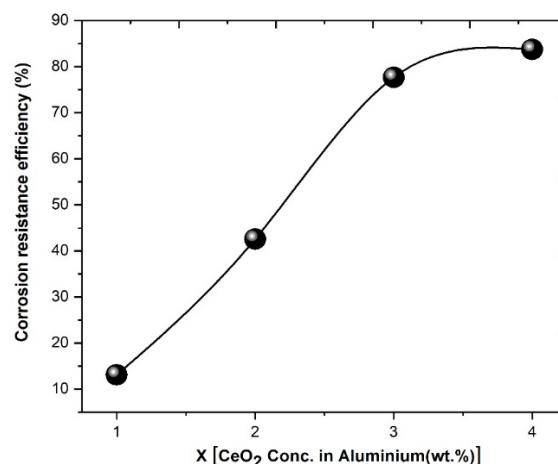


Figure 7(b). Variation of corrosion resistance efficiency of Al-CeO₂ MMNCs with different CeO₂ concentration

CONCLUSIONS

CeO₂ nanoparticles were reinforced into the Al metal matrix for the fabrication of metal matrix nanocomposite by powder metallurgy method. The ceria nanoparticles were synthesized by using the Co-precipitation technique with an average crystallite size of 12.08 nm. The hardness of the nanocomposite was

improved due to ceria nanoparticles and a maximum hardness value of 96.6 HRB is observed for 2 wt. % CeO₂ in the Al metal matrix. The increase in hardness of the MMCs is attributed to the reduction in the dislocations present in the Al metal matrix due to uniform distribution of the ceria nanoparticles in the metal matrix. However, Al-CeO₂ nanocomposites suffer more wear as compared to pure Al metal, due to debris formed during the wear test which further acts as an abrasive particle to both the surfaces. The corrosion resistance of Al-CeO₂ MMNCs also improves by increasing the concentration of CeO₂ nanoparticles. The corrosion resistance efficiency is obtained as 13.10 %, 42.58 %, 77.67 %, and 83.75 % for the 1 wt.%, 2 wt.%, 3 wt.%, and 4 wt.% ceria concentration, respectively. Thus, Al-CeO₂ MMNCs show better mechanical and corrosion resistance properties than pure Al metal which makes it suitable for marine technology applications.

ACKNOWLEDGMENT

Naveen Kumar is thankful to the MHRD, Government of India, and Director, MANIT for providing fellowship and infrastructure to carry out this research work.

REFERENCES

1. R. Casati, M. Vedani. Metal matrix composites reinforced by nanoparticles—a review. *Metals* **2014**, 4, 65-83.
2. Y.-H. Choa, J.-K. Yang, B.-H. Kim, Y.-K. Jeong, J.-S. Lee, T. Nakayama, T. Sekino, K. Niihara. Preparation and characterization of metal/ceramic nanoporous nanocomposite powders. *J. Magnetism Magnetic Mater.* **2003**, 266, 12-19.
3. E.-S. Yoon, J.-S. Lee, S.-T. Oh, B.-K. Kim. Microstructure and sintering behavior of W-Cu nanocomposite powder produced by thermo-chemical process. *Int. J. Refractory Metals Hard Materials* **2002**, 20, 201-06.
4. A. Contreras, V. Lopez, E. Bedolla. Mg/TiC composites manufactured by pressureless melt infiltration. *Scripta Materialia* **2004**, 51, 249-53.
5. W.D. Callister. *Materials science and engineering an introduction*, John Wiley, **2007**.
6. N. Chawla, Y.L. Shen. Mechanical behavior of particle reinforced metal matrix composites. *Adv. Engine. Mater.* **2001**, 3, 357-70.
7. G. Moona, R. Walia, V. Rastogi, R. Sharma. Aluminium metal matrix composites: A retrospective investigation. *Ind. J. Pure Appl. Phys. A* **2018**, 56, 164-75.
8. M.T. Alam, A.H. Ansari, S. Arif, M.N. Alam. Mechanical properties and morphology of aluminium metal matrix nanocomposites-stir cast products. *Advances in Materials Processing Technologie* **2017**, 3, 600-615.
9. F. Khalid, O. Beffort, U. Klotz, B. Keller, P. Gasser, S. Vaucher. Study of microstructure and interfaces in an aluminium-C60 composite material. *Acta Materialia* **2003**, 51, 4575-82.
10. C. Kwangmin, S. Jiyeon, B. Donghyun, C. Hyunjo. Mechanical properties of aluminum-based nanocomposite reinforced with fullerenes. *Transactions of Nonferrous Metals Soc. China* **2014**, 24, 47-52.
11. A. Mazahery, H. Abdizadeh, H. Baharvandi. Development of high-performance A356/nano-Al₂O₃ composites. *Materials Science Engineering: A* **2009**, 518, 61-64.
12. V. Tiku, K. Navin, R. Kurchania. Study of Structural and Mechanical Properties of Al/Nano-Al₂O₃ Metal Matrix Nanocomposite Fabricated by Powder Metallurgy Method. *Trans. Ind. Institute of Metals* **2020**, 1-7.
13. K.K. Alaneme, K.O. Sanusi. Microstructural characteristics, mechanical and wear behaviour of aluminium matrix hybrid composites reinforced with alumina, rice husk ash and graphite. *Engin. Sci. Techn., Int. J.* **2015**, 18, 416-22.
14. Y. Huang, P. Bazarnik, D. Wan, D. Luo, P.H.R. Pereira, M. Lewandowska, J. Yao, B.E. Hayden, T.G. Langdon. The fabrication of graphene-reinforced Al-based nanocomposites using high-pressure torsion. *Acta Materialia* **2019**, 164, 499-511.
15. C. Wu, R. Shi, G. Luo, J. Zhang, Q. Shen, Z. Gan, J. Liu, L. Zhang. Influence of particulate B₄C with high weight fraction on microstructure and mechanical behavior of an Al-based metal matrix composite. *J. Alloys Comp.* **2019**, 789, 825-33.
16. K. Pal, K. Navin, R. Kurchania. Study of structural and mechanical behaviour of Al-ZrO₂ metal matrix nanocomposites prepared by powder metallurgy method. *Materials Today: Proceedings* **2020**.
17. V. Bhattacharya, K. Chattopadhyay. Microstructure and wear behaviour of aluminium alloys containing embedded nanoscaled lead dispersoids. *Acta Materialia* **2004**, 52, 2293-304.
18. C. Yan, W. Lifeng, R. Jianyue. Multi-functional SiC/Al composites for aerospace applications. *Chinese Journal of Aeronautics* **2008**, 21, 578-84.
19. J.Z. Liao, M.J. Tan, A. Santoso In *Advanced Materials Research* **2011**, 311, 80-83.
20. C. Vargel. *Corrosion of aluminium*, Elsevier, **2020**.
21. H. Ezuber, A. El-Houd, F. El-Shawesh. A study on the corrosion behavior of aluminum alloys in seawater. *Materials Design* **2008**, 29, 801-05.
22. M. Keddad, C. Kuntz, H. Takenouti, D. Schustert, D. Zuili. Exfoliation corrosion of aluminium alloys examined by electrode impedance. *Electrochimica Acta* **1997**, 42, 87-97.
23. Q.L. Zhang, Z.M. Yang, B.J. Ding In *Materials Science Forum* **2009**, 610, 233-38.
24. S. Sebastianm, A.L. Fathima, V. Shally, G. Jayam. Effect of Calcination Temperature on Pure Cerium Oxide Nanoparticles by Precipitation Method. *Materials Science Forum* **2009**, 6, 23.
25. L. Mädler, W.J. Stark, S.E. Pratsinis. Flame-made ceria nanoparticles. *J. Mater. Res.* **2002**, 17, 1356-62.
26. H. Yang, C. Huang, A. Tang, X. Zhang, W. Yang. Microwave-assisted synthesis of ceria nanoparticles. *Mater. Res. Bull.* **2005**, 40, 1690-95.
27. T. Masui, H. Hirai, N. Imanaka, G. Adachi, T. Sakata, H. Mori. Synthesis of cerium oxide nanoparticles by hydrothermal crystallization with citric acid. *J. Mater. Sci. Lett.* **2002**, 21, 489-91.
28. M. Qian, G. Schaffer In *Sintering of advanced materials*; Elsevier: **2010**, pp 291-323.
29. A. Korchef, Y. Champion, N.J. Njah. X-ray diffraction analysis of aluminium containing Al₈Fe₂Si processed by equal channel angular pressing. *Journal of Alloys Compounds* **2007**, 427, 176-82.
30. S.A. Sajjadi, H. Ezatpour, H. Beygi. Microstructure and mechanical properties of Al-Al₂O₃ micro and nano composites fabricated by stir casting. *Materials Science Engineering: A* **2011**, 528, 8765-71.
31. G.V. Kumar, C. Rao, N. Selvaraj. Mechanical and tribological behavior of particulate reinforced aluminum metal matrix composites—a review. *J. Minerals Mater. Characterization Engineering* **2011**, 10, 59.
32. E. McCafferty. Validation of corrosion rates measured by the Tafel extrapolation method. *Corrosion Sci.* **2005**, 47, 3202-15.
33. D.V. Jamkar, B.J. Lokhande, S.B. Kondawar. Improved electrochemical performance of free standing electrospun graphene incorporated carbon nanofibers for supercapacitor. *J. Mat. NanoSci.* **2019**, 6, 32-37.
34. B.S. Chhikara, R.S. Varma. Nanochemistry and nanocatalysis science: Research advances and future perspectives. *J. Mat. NanoSci.* **2019**, 6, 1-6.
35. P.M. Ashraf, S. Shibli. Reinforcing aluminium with cerium oxide: A new and effective technique to prevent corrosion in marine environments. *Electrochem. Commun.* **2007**, 9, 443-48.
36. Y. Lu, M. Ives. The improvement of the localized corrosion resistance of stainless steel by cerium. *Corrosion Sci.* **1993**, 34, 1773-85.